

# MIMO Vibration Test Design for BARC Challenge Problem

Brandon Zwink, Kevin Cross, and Deborah Fowler

Sandia National Laboratories\*  
Albuquerque, NM 87185

## 1 ABSTRACT

The case study of the Box Assembly with Removable Component (BARC) challenge problem is utilized to demonstrate an approach to vibration test design for structure-born vibration on a component. Four design concepts are demonstrated and analytical results show how a laboratory vibration fixture can be optimized to minimize the forces required to perfectly replicate a reference field environment response of a component. The methods utilized in this paper focus on achieving the appropriate number of excitation and response degrees of freedom which results in replicating the field environment forces that act on the component in a laboratory test setup with different boundary conditions. Ultimately, a vibration test stand is proposed that is capable of applying this concept experimentally using electro-dynamic shakers.

**Keywords:** MIMO, Vibration, BARC, FINE, ICE

---

\*Sandia National Laboratories is a multi-mission laboratory managed and operated by National Technology and Engineering Solutions of Sandia, LLC, a wholly owned subsidiary of Honeywell International, Inc., for the U.S. Department of Energy's National Nuclear Security Administration under contract DE-NA-0003525.

## 2 NOMENCLATURE

Table 1: List of nomenclature

Symbol	Description
$x$	Displacement (time domain)
$X$	Displacement (frequency domain)
$f$	Force (time domain)
$F$	Force (frequency domain)
$U$	Mode shapes (eigenvectors)
$M$	Mass
$\zeta$	Damping ratio ( $\frac{\text{damping}}{\text{critical damping}}$ )
$j$	Imaginary number ( $\sqrt{-1}$ )
$\omega$	Frequency
$\omega_k$	Natural frequency for the $k^{\text{th}}$ mode
$\bullet_i$	Response degree of freedom
$\bullet_j$	Excitation degree of freedom
$\bullet_k$	$k^{\text{th}}$ mode
$\bullet$	Value is in modal domain
$\ddot{\bullet}$	Second derivative with respect to time, e.g. acceleration
$\{\bullet\}$	Denotes vector
$[\bullet]$	Denotes matrix
$[\bullet]^T$	Transpose of a matrix
$[\bullet]^\dagger$	Pseudo-inverse of a matrix

## 3 INTRODUCTION

Replicating field vibration environments in a laboratory setting is utilized in the aero-space community to ensure proper function of components under extreme conditions. The Box Assembly with Removable Component (BARC) challenge problem [1] was introduced to the structural dynamics community as a challenge to replicate complex boundary conditions and excitations in a laboratory. This paper demonstrates how application of the Intrinsic Connection Excitation (ICE) [2] methodology can be utilized to solve the BARC challenge problem. An optimized analytical solution is then utilized to create an experimental test design.

An image of the BARC finite element model (FEM) is shown in Figure 1. The design iteration of the BARC utilized in this study is the split-box design as it is an exaggeration of the demonstrated problem in which the boundary condition of the removable component (or bench) is flexible relative to the stiffness of the component being tested. Traditional component vibration tests often incorporate the assumption that the boundary conditions of the component being tested are stiff relative to the component and the challenge problem was introduced with the hope of learning how to conduct an accurate vibration test when the stiff boundary condition assumption is invalid.

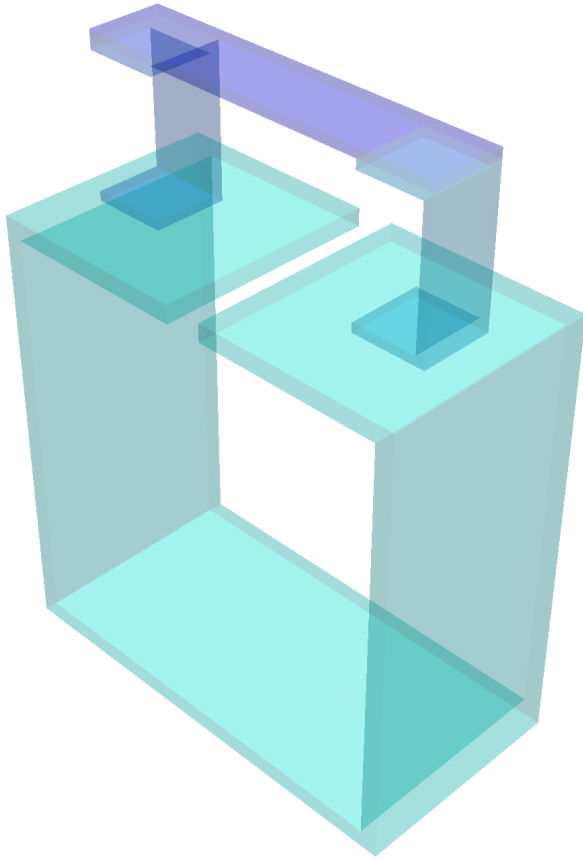


Figure 1: Box Assembly with Removable Component Finite Element Model (Box in Green and Removable Component in Blue).

#### 4 REFERENCE FIELD ENVIRONMENT

The BARC challenge problem definition suggests a reference field environment created by an impulse excitation on the side of the box section of the BARC. Therefore, an impulse excitation was generated in the time domain using a 2000 Hz half-sine wave and applied to the location specified on the side of the box in the challenge problem description. The time history for the generated impulse signal, the frequency spectra for the generated impulse, and the location on the side of the box where the impulse was applied to the finite element model are all shown in Figure 2. The width of the pulse was tuned to ensure a broad excitation bandwidth to excite many modes of the reference structure ensuring the intent of the challenge problem of having a complicated excitation of the component was met.

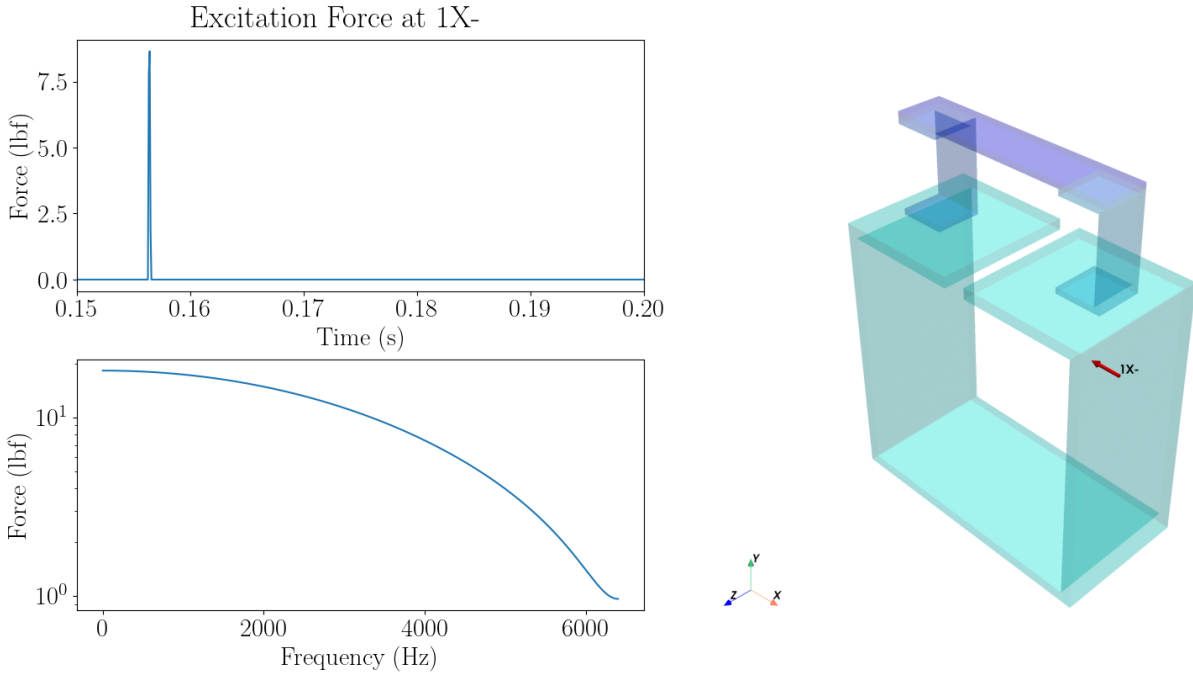


Figure 2: Reference Excitation for BARC Field Configuration (DOF 1X- depicted with a red arrow).

In general, all calculations were done in the frequency domain. Care was taken to ensure that the time window was long enough to capture the entire excitation/response to avoid leakage issues by increasing the damping in the system and increasing the length of the time window. A time window of 10 seconds was utilized and sample rate of 12800 Hz was chosen to sufficiently capture the active dynamics from the 2000 Hz impulse. A two percent modal damping was assumed for all modes of the finite element model to help the response die out within the time window. Additionally, the 6 rigid body modes for the system were modified to have a natural frequency of 10 Hz instead of 0 Hz which effectively provides a soft boundary condition for the structure instead of a completely free boundary condition. This was done to limit the displacement of the structure to a reasonable range so the response could be easily visualized in an animation. The Fourier transform and inverse Fourier transform were utilized to convert between frequency and time domain as needed. The first step in computing the response of the structure was to synthesize the modal frequency response functions for each of the 100 modes of the finite element model. The 100 synthesized frequency response functions, one for each mode of the system, were then populated diagonally to form the complete modal frequency response function matrix for the entire system. Each diagonal term of the modal frequency response function matrix was calculated as shown in Equation 1.

$$\{\ddot{H}_k\} = \frac{\ddot{X}_i}{\bar{F}_j} = \frac{-\{\omega\}^2}{\bar{M}_k(-\{\omega\}^2 + 2j\omega_k\xi_k\{\omega\} + \omega_k^2)} \quad (1)$$

The system modal frequency response function matrix can then be utilized to compute the response of the system, in the frequency domain, as shown in Equation 2. For reference, brackets are shown to depict which parts of Equation 2 constitute the modal acceleration and modal force.

$$\{\ddot{X}_i\} = [U_i] \underbrace{\begin{bmatrix} \{\ddot{H}_{k_1}\} & 0 & 0 & \dots \\ 0 & \{\ddot{H}_{k_2}\} & 0 & \dots \\ 0 & 0 & \{\ddot{H}_{k_3}\} & \\ \vdots & \vdots & & \ddots \\ & & & \{\ddot{H}_{k_n}\} \end{bmatrix}}_{\{\ddot{X}\}} \underbrace{[U_j]^T \{F_j\}}_{\{\ddot{F}\}} \quad (2)$$

Once the physical response of the system is calculated in the frequency domain using Equation 2, the physical response can be converted back into the time domain using the inverse Fourier transform. An example of the acceleration response calculated on

the component for the reference field environment is given shown in Figure 3. In general, the peak response of the component to the provided excitation was on the order of about 20 g's of response acceleration.

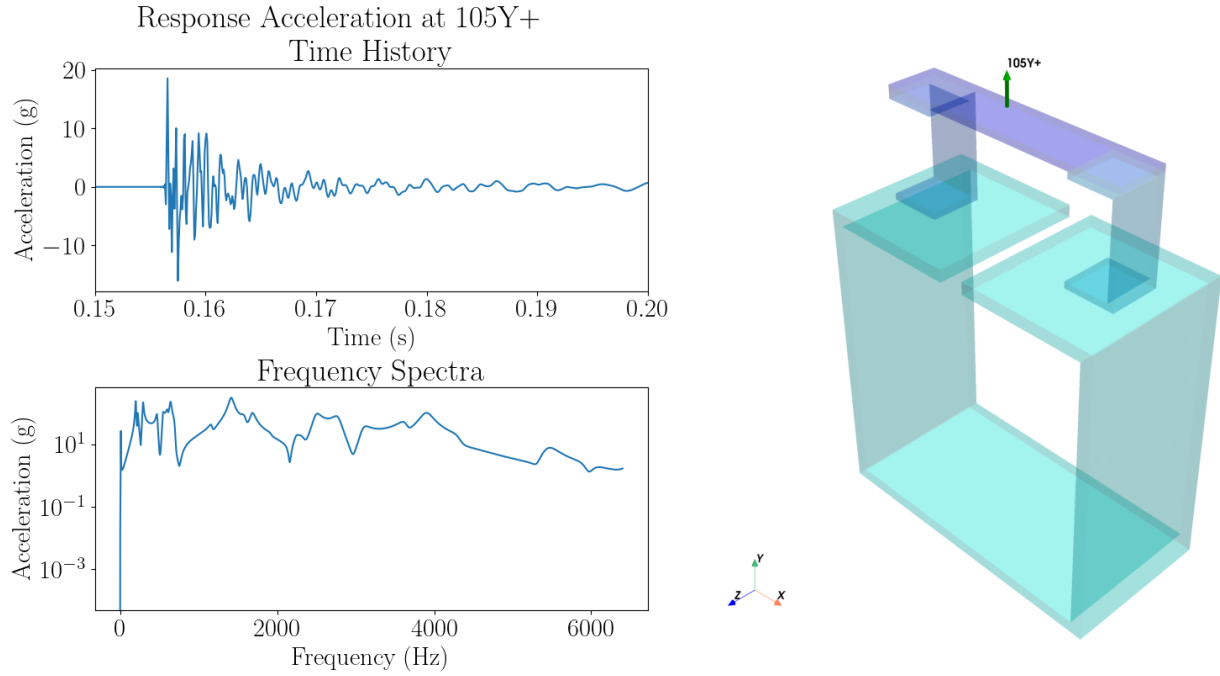


Figure 3: Field response at 105Y+ (DOF 105Y+ depicted with a green arrow).

## 5 ANALYSIS

The method utilized to analyze and design a vibration test capable of replicating a complicated field environment response was derived from Zwink [2]. The method was referred to as Intrinsic Connection Excitation (ICE), and results in a multiple-input-multiple-output (MIMO) style test based on the rank of the excitation of the component being tested. In general, ICE methodology was based on the work by Reyes [3] and defines the rank of the excitation as the number of boundary condition forces acting on the component being tested. A test capable of replicating the field environment for the component is then created by utilizing as many or more forces and as many or more response degrees of freedom as the number of connection forces. This method is similar to the Impedance Matched Multi-Axis Test (IMMAT) methodology developed by Daborn [4]. Data for this work was processed using the Structural Dynamics Python Library developed by Rohe [5].

The main difference between the methodology utilized in this paper and the IMMAT methodology is that no attempt is made to match the impedance of the next level assembly and instead the vibration fixture is designed to be as light and stiff as possible and the shakers are relied upon to match the boundary condition forces of the field environment.

A six step process is demonstrated to develop and evaluate a vibration test capable of replicating complex field environments and is each step is explained in the following sections. The six steps are given as follows:

1. Simplify Boundary Condition Forces
2. Compute Boundary Condition Forces and Moments (Optional)
3. Design Vibration Test Fixture to Apply Boundary Condition Forces
4. Compute Fixture Forces
5. Compute Component Response to Fixture Forces
6. Design Vibration Test Stand

## 5.1 Simplify Boundary Condition Forces

The first step in the analysis is to define the boundaries of the component and identify the boundary condition forces that act across that boundary. For the BARC challenge problem, this boundary had been defined as the "bench" part of the assembly. This process can also involve making assumptions about the boundary condition forces acting on the component (or bench) to simplify and minimize the number of boundary condition forces thereby reducing the complexity of the test. In this case, an assumption was made to reduce the rank and complexity of the boundary condition forces. For example, the boundary condition forces could be approximated as two sets of six degree of freedom forces acting on the base of each leg of the component (three translation and three rotational forces at each location). This assumption results in a total of 12 degrees of freedom of excitation for the component and are depicted in Figure 4. For the example of the BARC hardware, there are actually a total of 8 bolts (4 on each leg) attaching the bench to the box. Effectively, an assumption was made to simplify the 4 bolt connection at each leg of the bench a single six degree of freedom connection point instead of including six connection degrees of freedom for each of the four bolts on each leg. This assumption was based on the mode shapes of the BARC and the excitation bandwidth for this study. There is a frequency at which this assumption will become invalid as the feet of the bench demonstrate elasticity, but as this was not observed in the mode shapes until far outside of the excitation bandwidth, it was assumed this simplification was valid for this study.

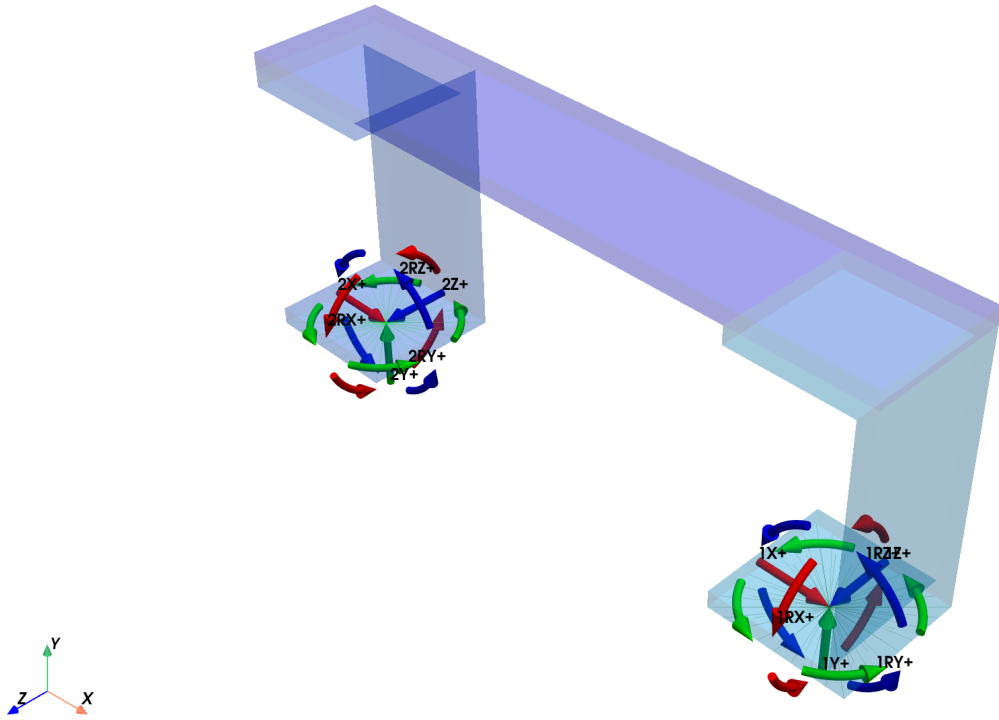


Figure 4: 12 Boundary Condition Forces Acting on Component. Three translation and three rotational forces at two locations.

## 5.2 Compute Boundary Condition Forces and Moments (Optional)

The field response on the component along with its associated model can be utilized to compute the boundary condition forces and moments acting on the feet of the component. This step is optional, but informative in determining the magnitude of the forces that need to be applied to the component to replicate the field response in absence of a test fixture. For instance, the magnitude of the boundary condition forces can inform the general size of electro-dynamic shaker or the length of moment

arm needed to achieve a specified moment at the connection degree of freedom. The forces at the boundary condition degrees of freedom can be computed using Equation 3 while utilizing the mode shapes of the free boundary condition component and modal frequency response functions synthesized from the modes of the free boundary condition component. For this study, a subset of response degrees of freedom (shown in Figure 5) was chosen as opposed to utilizing all bench degrees of freedom. In general, only 12 response degrees of freedom are needed to solve for the 12 boundary condition forces (if the response locations are well conditioned to distinguish the connection forces across the frequency range of interest), but in this case a set of 18 was chosen to help ensure a well conditioned problem by creating an over-determined set of equations.

$$\{F_j\} = [[U_i][\ddot{H}][U_j]^T]^{\dagger}\{\ddot{X}_i\} \quad (3)$$

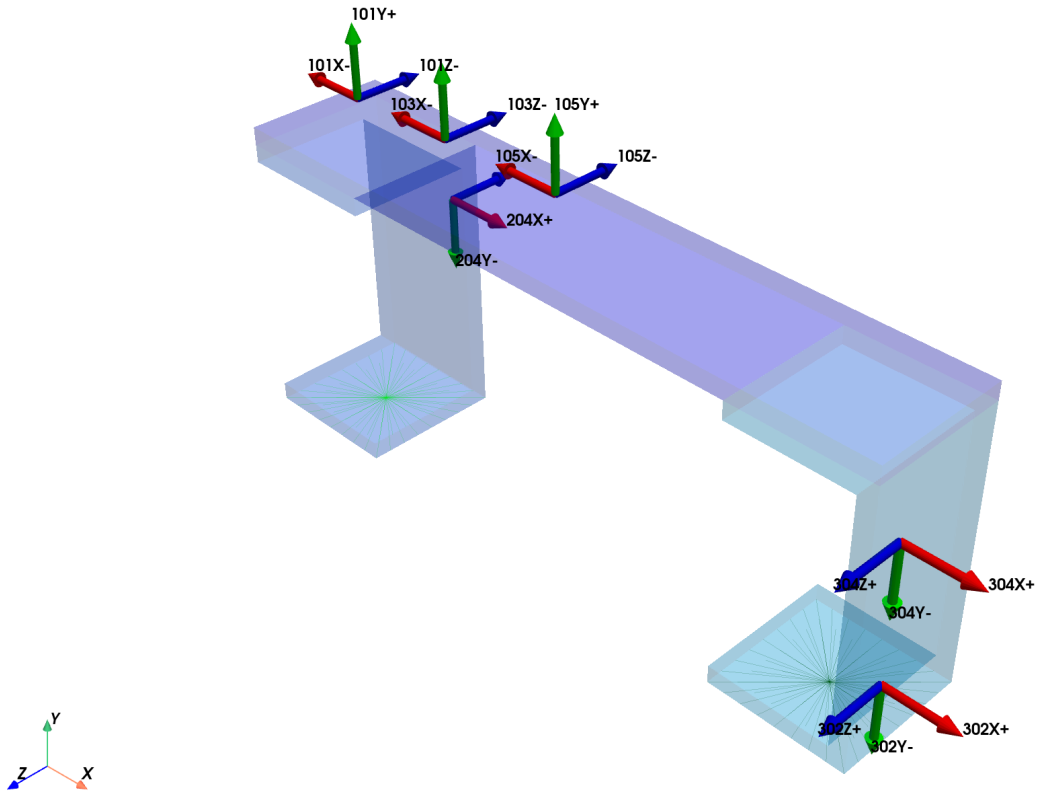


Figure 5: 18 Chosen Response Degrees of Freedom on the Component.

The resulting boundary condition forces on the free component are shown in Figures 6 through 17. Notice that these forces are roughly an order of magnitude smaller than the original excitation force used to excite the field assembly shown in Figure 2. So even when a large excitation is provided to a structure, it doesn't necessarily mean that large excitation forces are required to replicate the response on a component inside that structure.

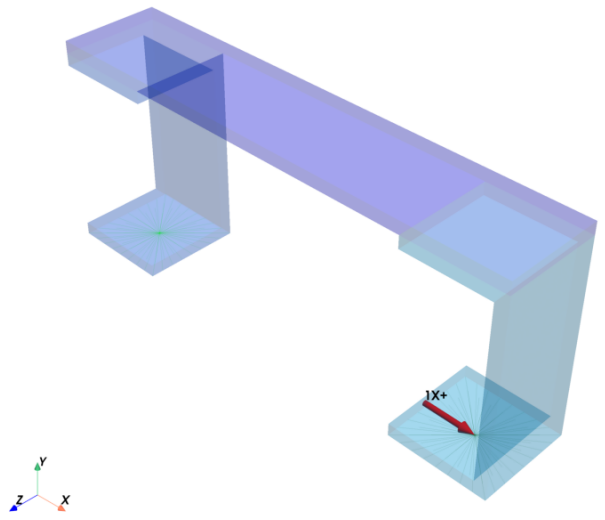
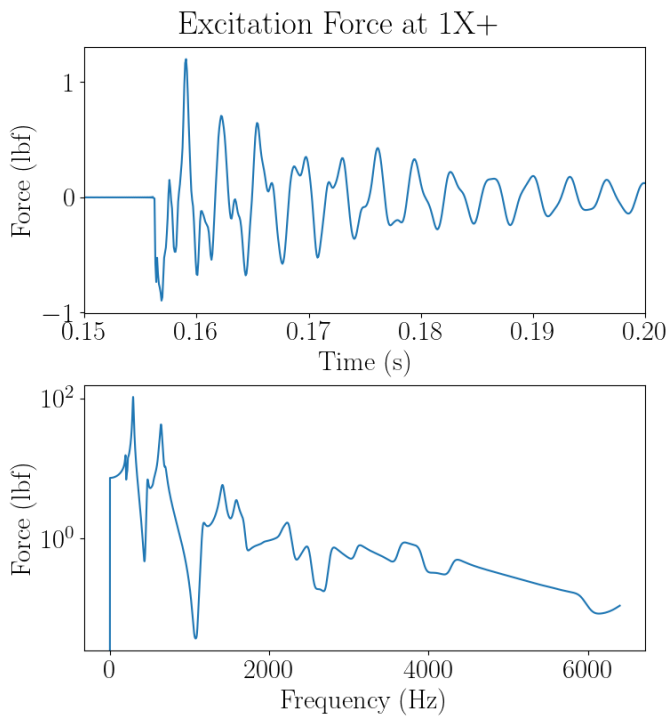


Figure 6: Boundary condition force at 1X+ (DOF 1X+ depicted with a red arrow).

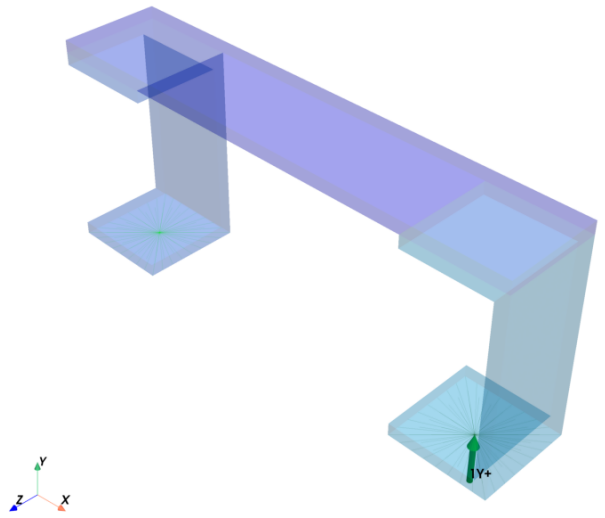
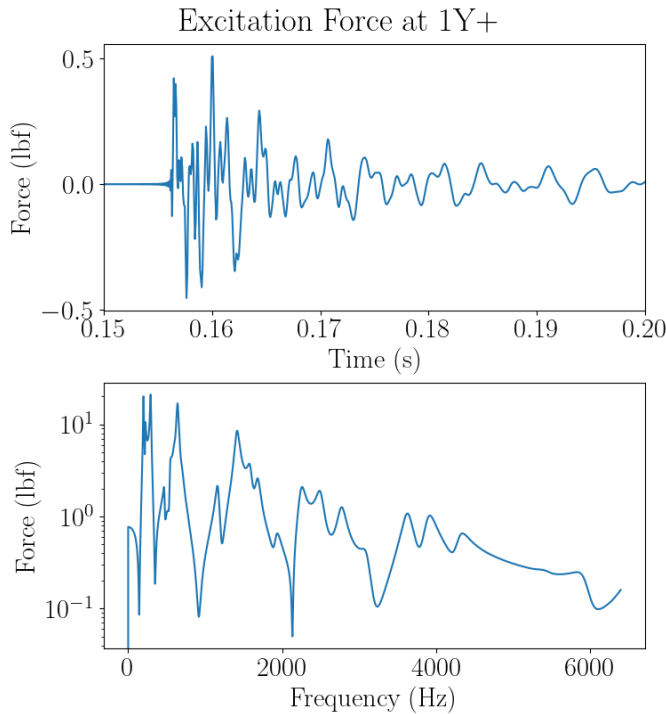


Figure 7: Boundary condition force at 1Y+ (DOF 1Y+ depicted with a green arrow).

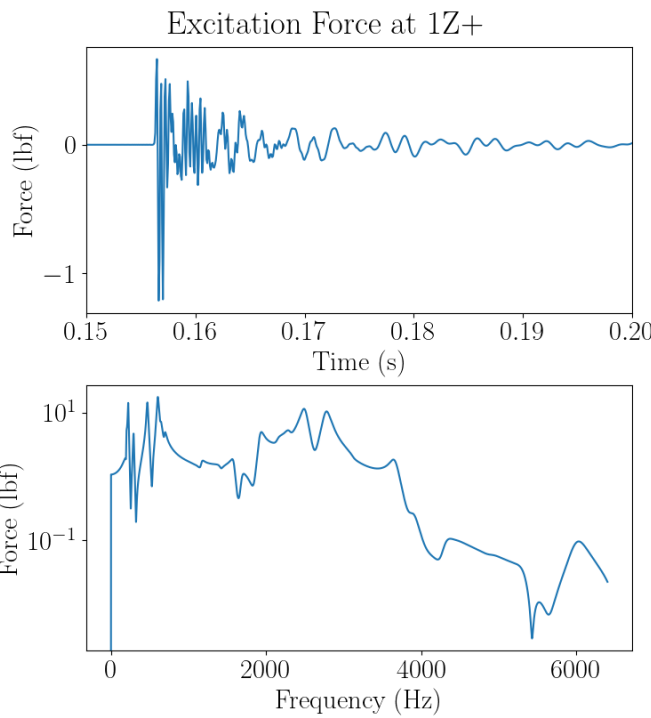


Figure 8: Boundary condition force at 1Z+ (DOF 1Z+ depicted with a blue arrow).

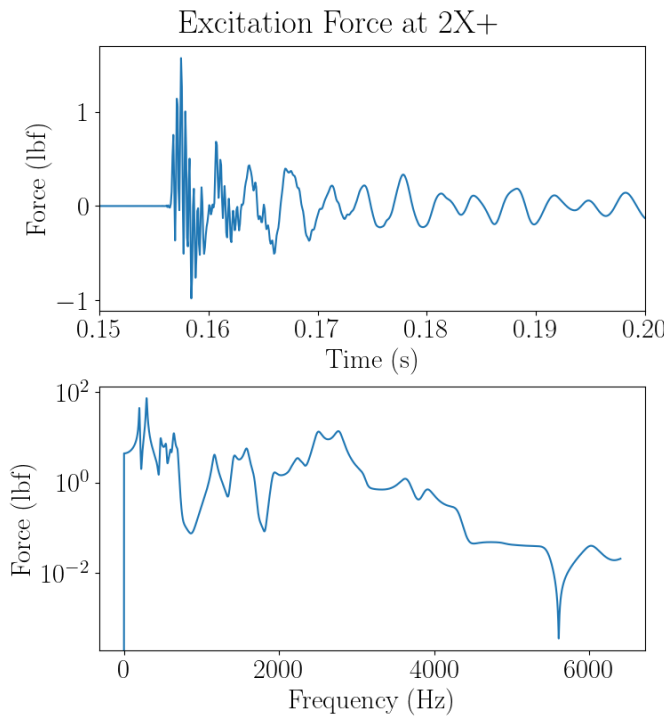


Figure 9: Boundary condition force at 2X+ (DOF 2X+ depicted with a red arrow).

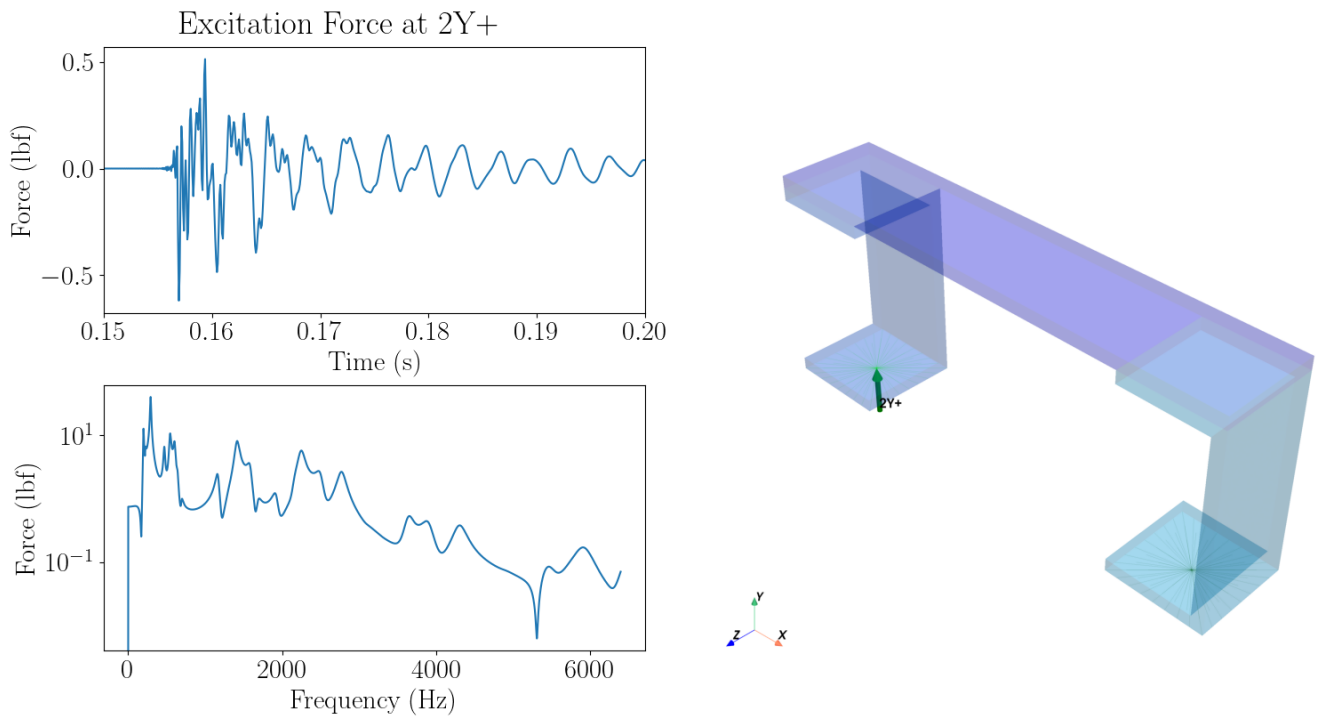


Figure 10: Boundary condition force at 2Y+ (DOF 2Y+ depicted with a green arrow).

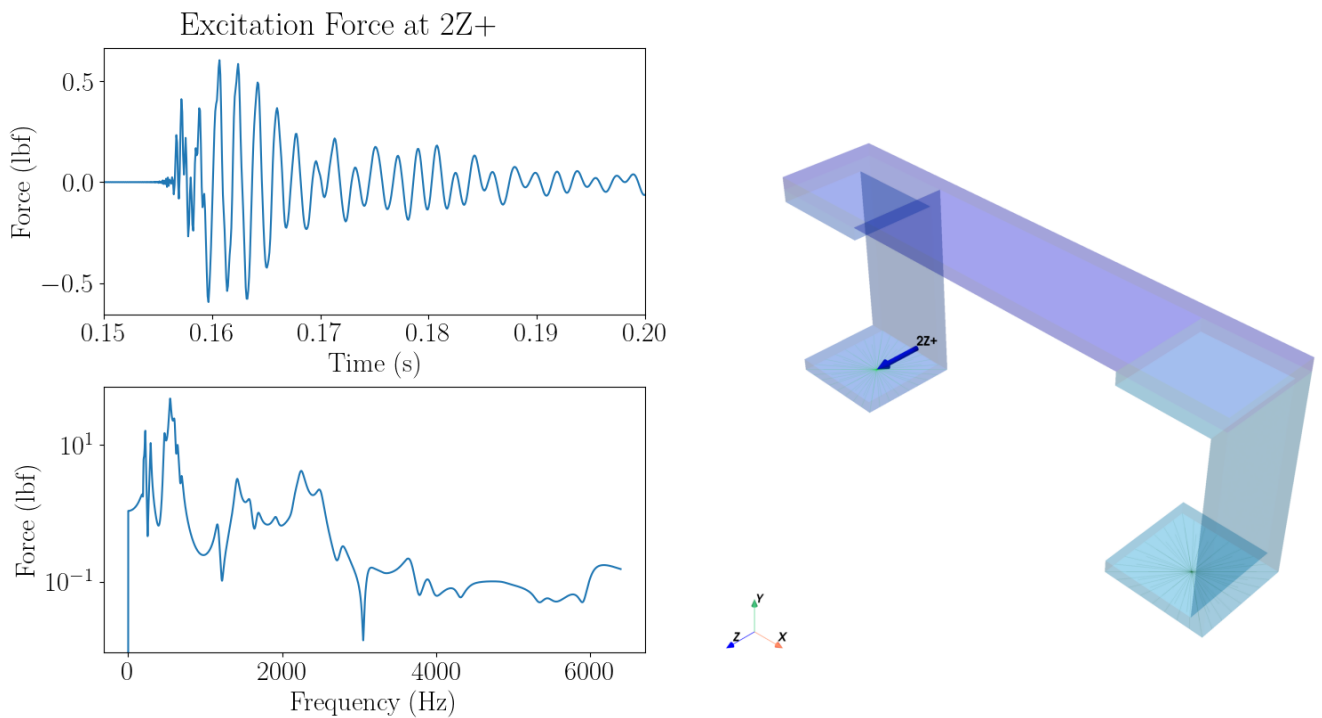


Figure 11: Boundary condition force at 2Z+ (DOF 2Z+ depicted with a blue arrow).

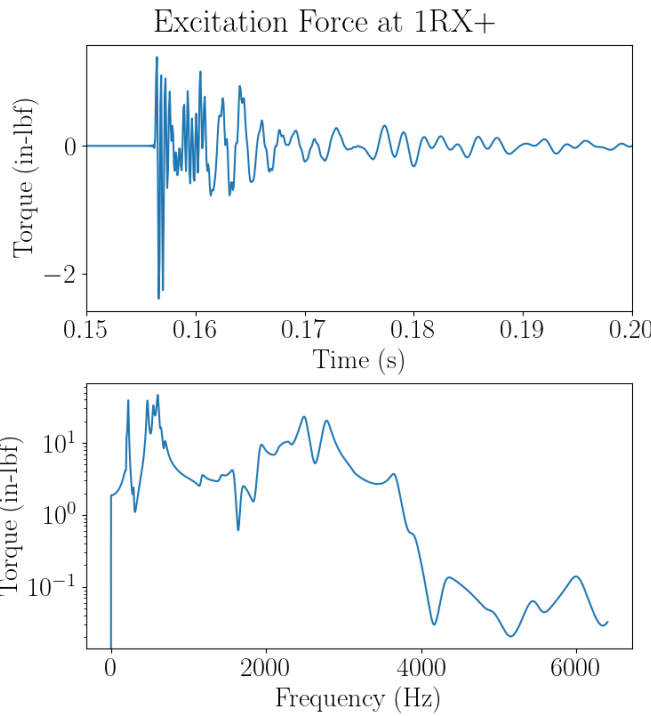


Figure 12: Boundary condition torque at 1X+ (Moment at 1X+ depicted with a red ring of arrows).

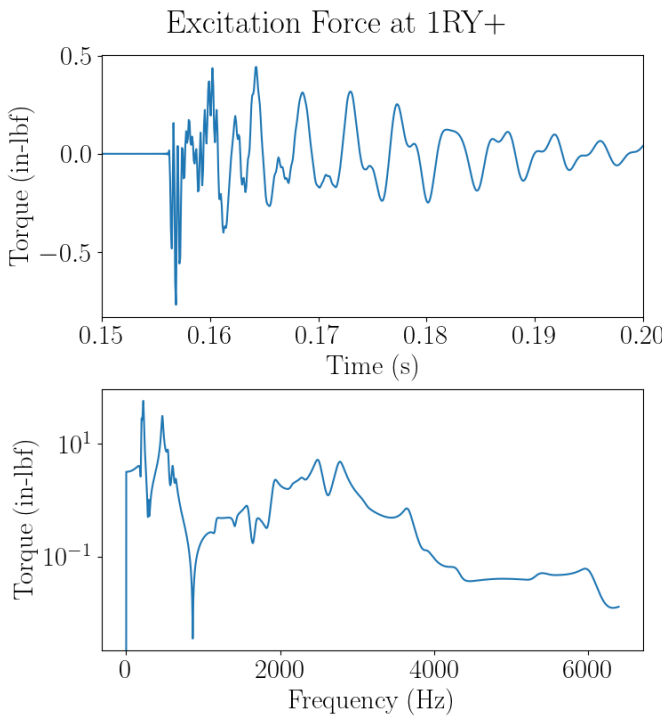


Figure 13: Boundary condition torque at 1Y+ (Moment at 1Y+ depicted with a green ring of arrows).

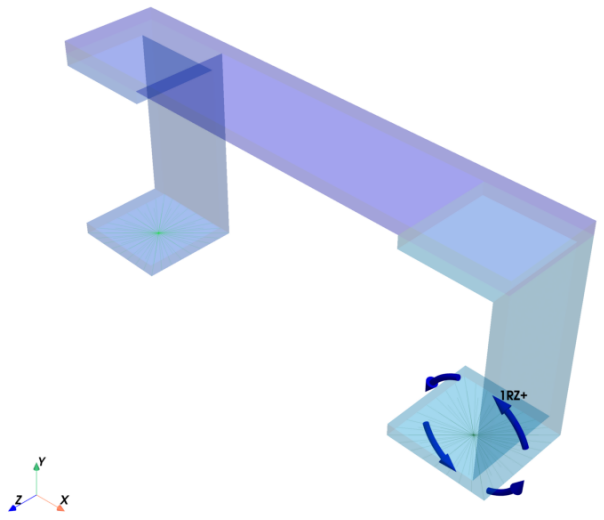
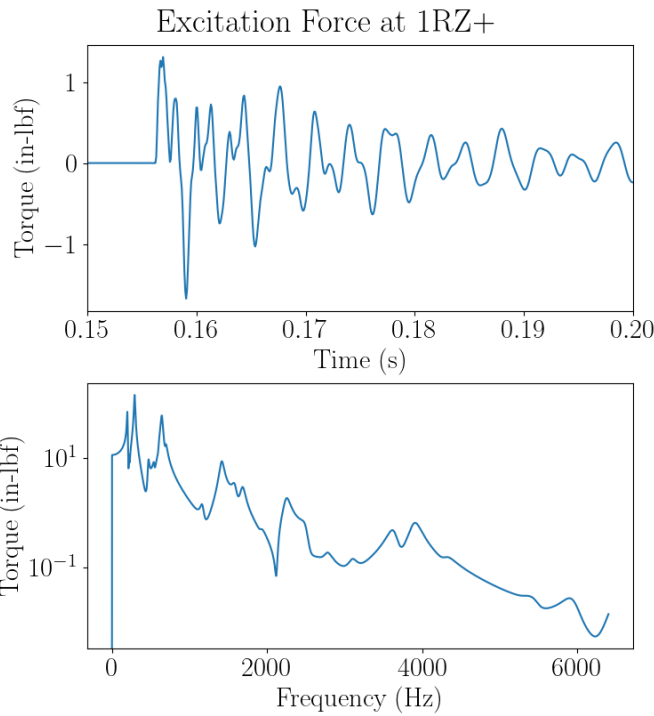


Figure 14: Boundary condition torque at 1Z+ (Moment at 1Z+ depicted with a blue ring of arrows).

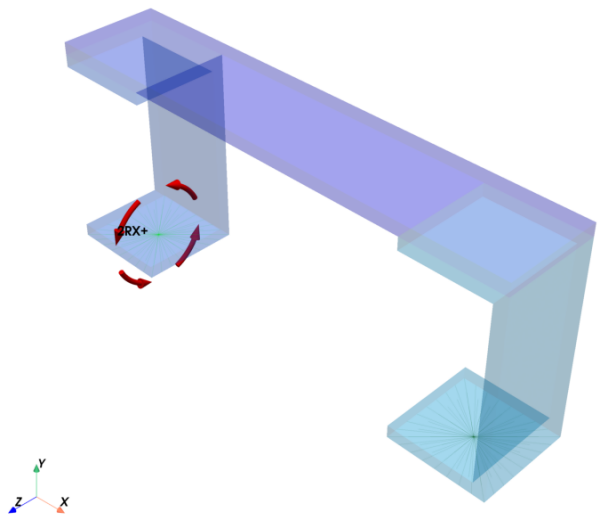
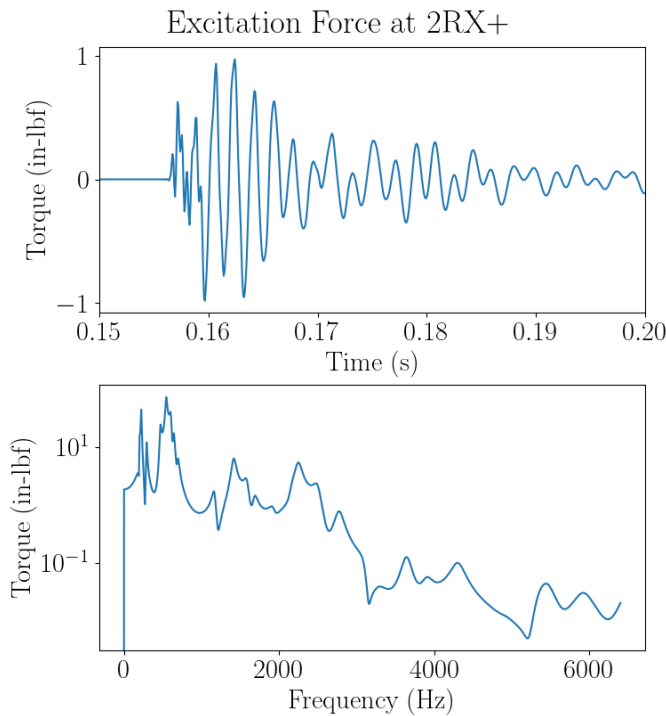


Figure 15: Boundary condition torque at 2X+ (Moment at 2X+ depicted with a red ring of arrows).

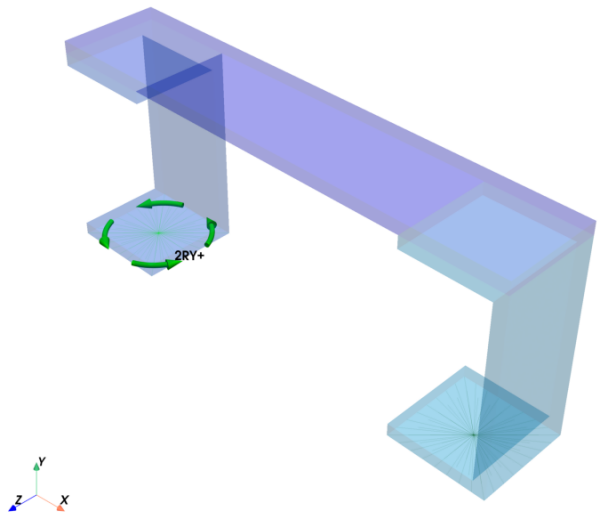
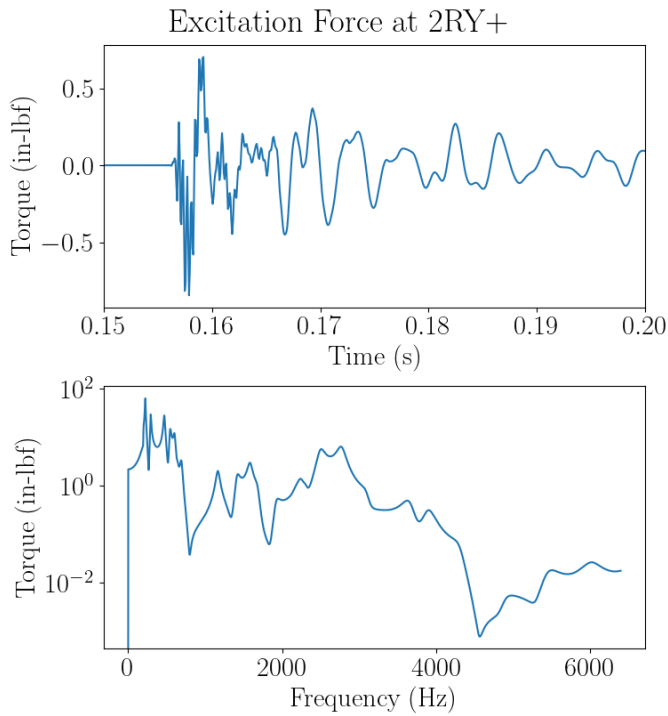


Figure 16: Boundary condition torque at 2Y+ (Moment at 2Y+ depicted with a green ring of arrows).

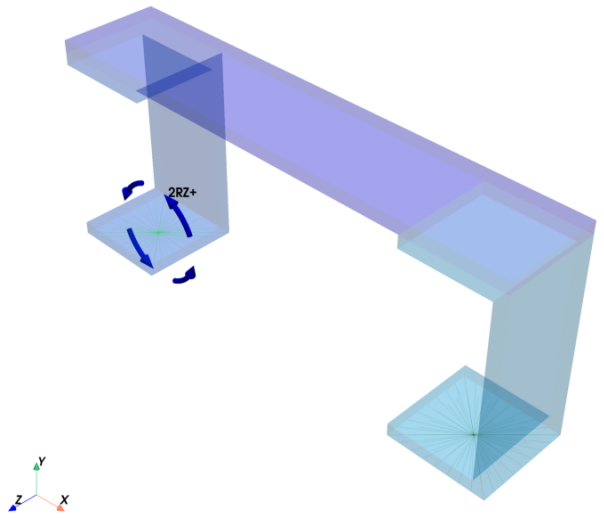
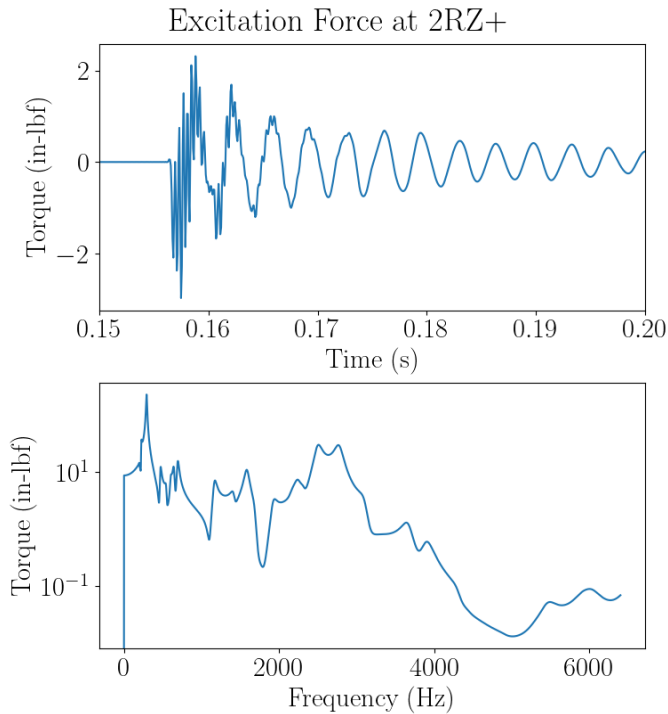


Figure 17: Boundary condition torque at 2Z+ (Moment at 2Z+ depicted with a blue ring of arrows).

### 5.3 Design Vibration Test Fixture to Apply Boundary Condition Forces

Now that the boundary condition forces are defined and understood, a vibration test fixture can be designed with the goal of applying these forces to the component as directly as possible. Multiple designs were tested analytically to demonstrate how optimizing the fixture to be lightweight and stiff in the directions in which forces are applied helps minimize the shaker forces required to replicate the environment. The designs tested were a poorly optimized single-plate design (shown in Figure 18), a moderately optimized dual-plate design (shown in Figure 19), an optimized design (shown in Figure 20), and an idealized solution (shown in Figure 4) in which the boundary condition forces could be applied directly to the component. Although not optimal, the single-plate design was included, for comparison purposes, as commercially available shaker systems typically incorporate a table base input. In general, engineering judgement was used to locate the forcing degrees of freedom with an effort to keep try to keep the shakers orthogonal to each-other and make them well conditioned to independently drive the connection forces shown in Figure 4.

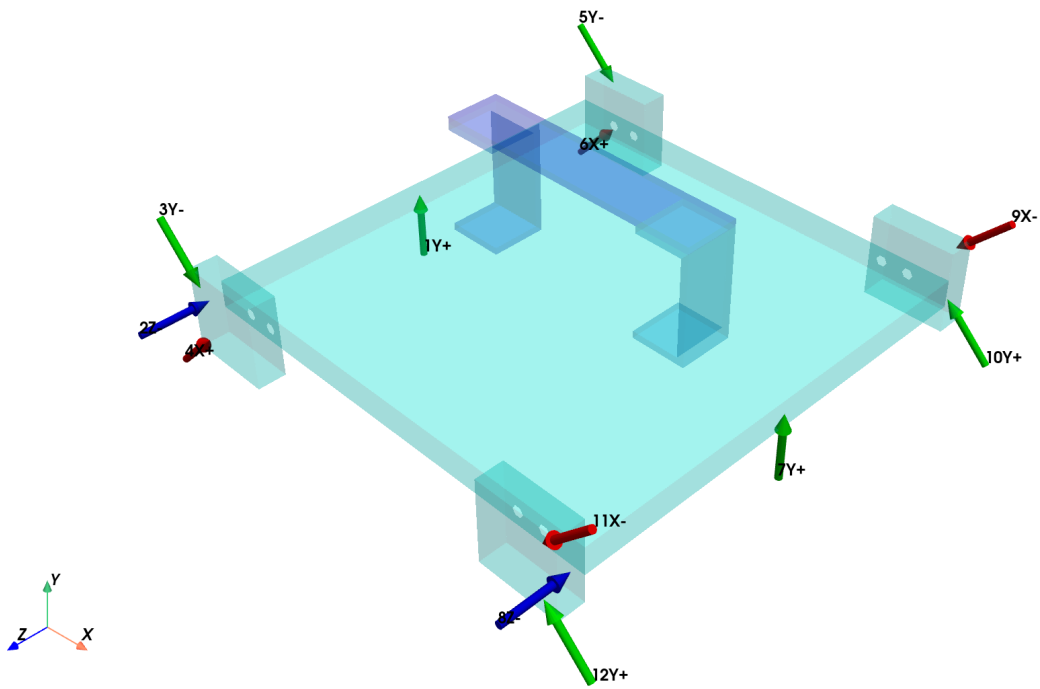


Figure 18: Single-plate fixture design with shaker excitation locations.

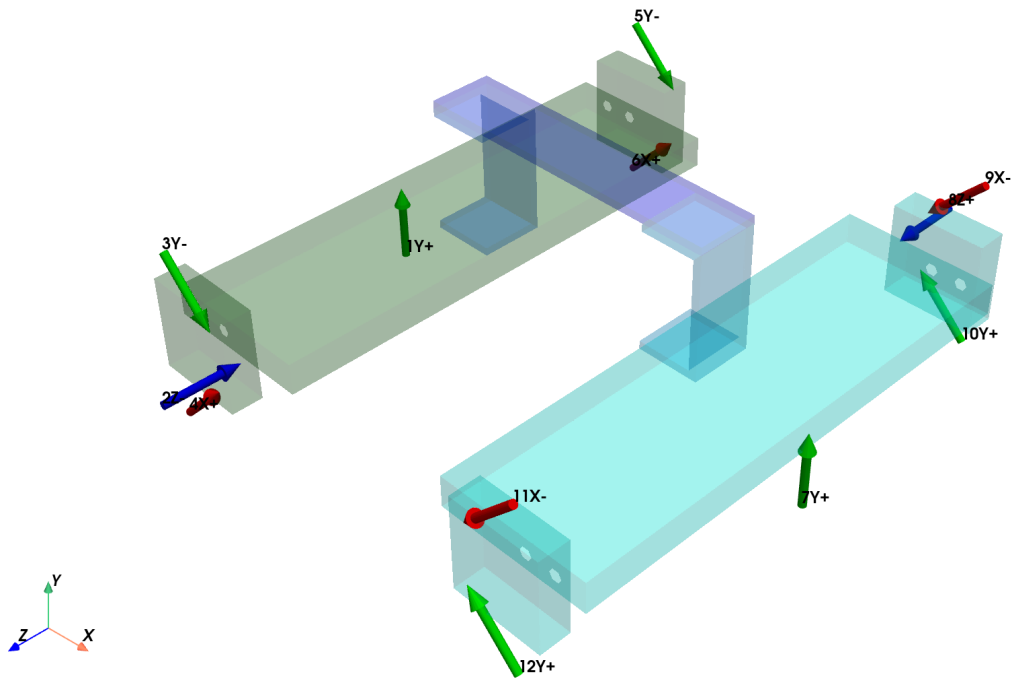


Figure 19: Dual-plate fixture design with shaker excitation locations.

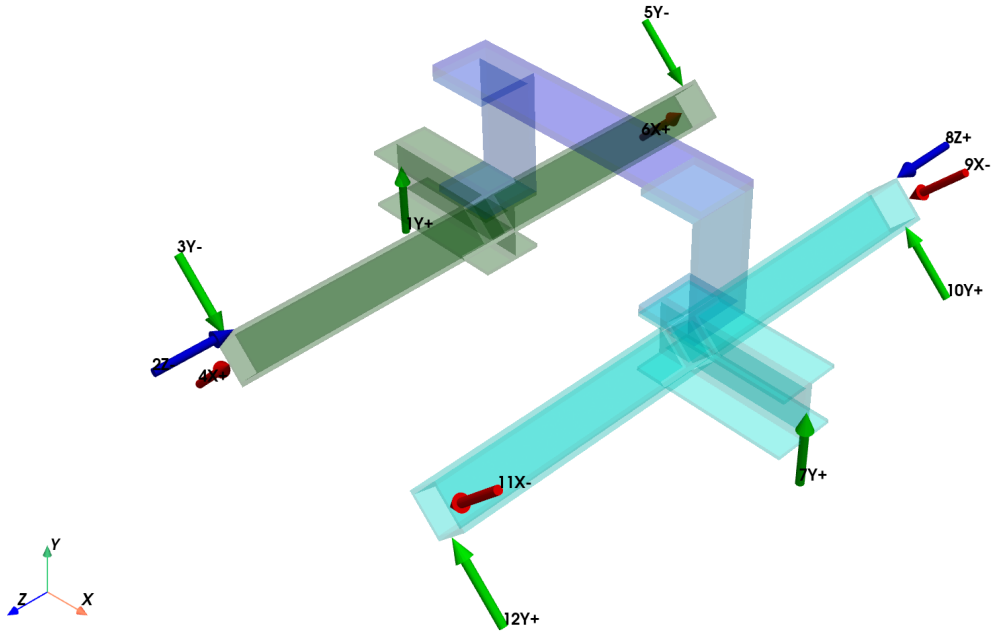


Figure 20: Optimized fixture design with shaker excitation locations.

#### 5.4 Compute Fixture Forces

The shaker forces required to achieve the reference component responses can be calculated using Equation 3. The maximum shaker force computed for each of the four designs are shown in Table 2.

Table 2: Maximum shaker force force for each design configuration.

Design	Max Force (lbf)
Reference BARC	8.65
Single-plate	4920.68
Dual-plate	22.32
Optimized	1.92
Component	1.57

The maximum shaker forces shown in Table 2, show that the maximum shaker force decreases as the fixture design becomes lighter and more stiff in applying the boundary condition forces to the component. The ideal case, in which there is no fixture results in the lowest shaker forces although it is not physically realizeable. The excitation force for the single plate design is especially high in part because the single plate fixture has more mass than the other designs and in part because the fixture plate must be bent to achieve the desired response of the component because each foot of the component moves somewhat independently.

## 5.5 Compute Component Response to Fixture Forces

The computed fixture forces can be applied to their respective finite element based modal models and component responses can be computed so they can be compared to the response of the component from the reference field environment configuration. The response of the component on each fixture can be computed using Equation 2. The resulting responses on the component at degree-of-freedom 105Y+ are shown for the single plate design in Figure 21, the dual-plate design in Figure 22, the optimized design in Figure 23, and the idealized component-only response in Figure 24. All designs resulted in nearly line-on-line response replication compared to the reference response as this is an analytical study in which infinite force can be applied to the fixture and all the designs adhered to the ICE design criteria of having as many or more excitation degrees of freedom and response control degrees of freedom as there were assumed connection degrees of freedom to the component.

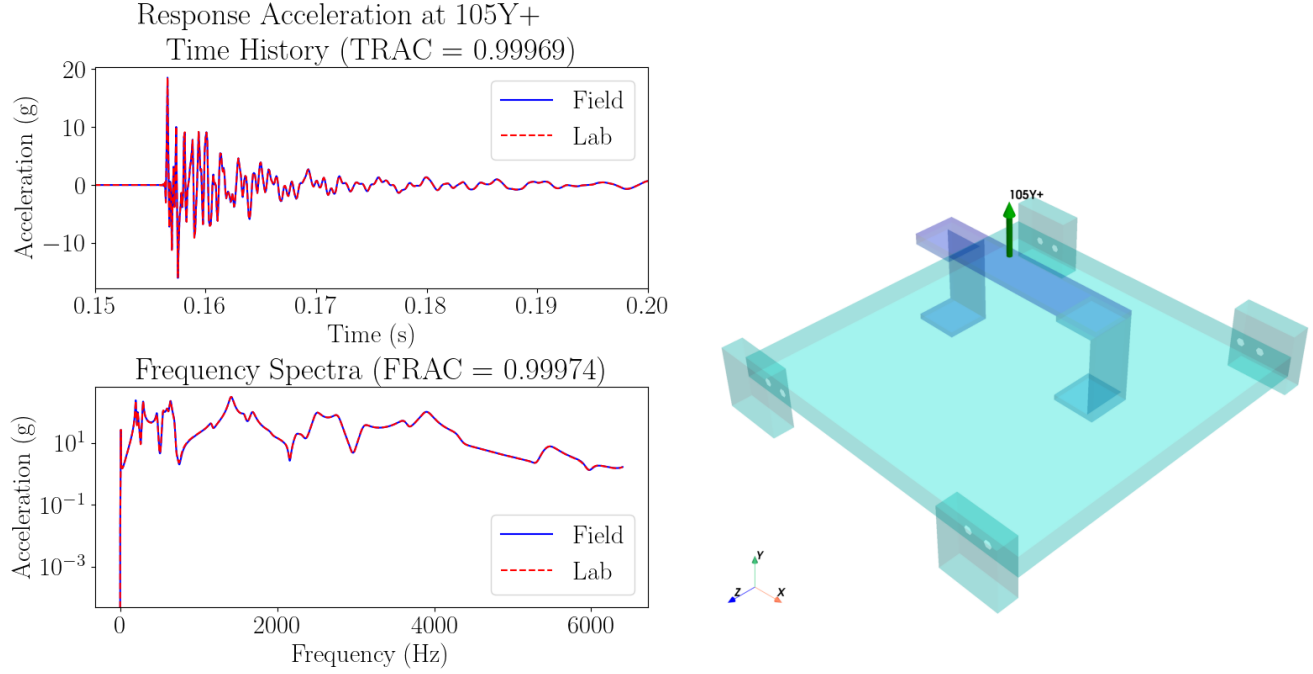


Figure 21: Single-plate response at 105Y+ compared to reference response.

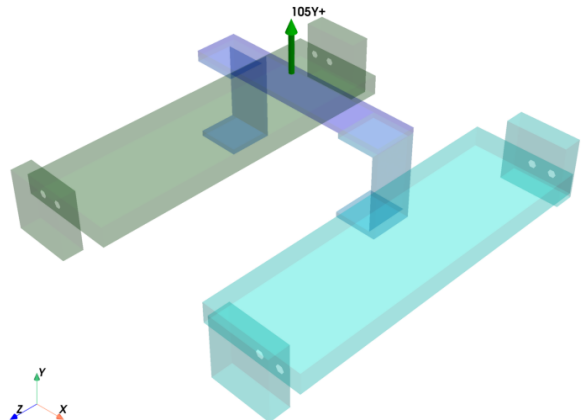
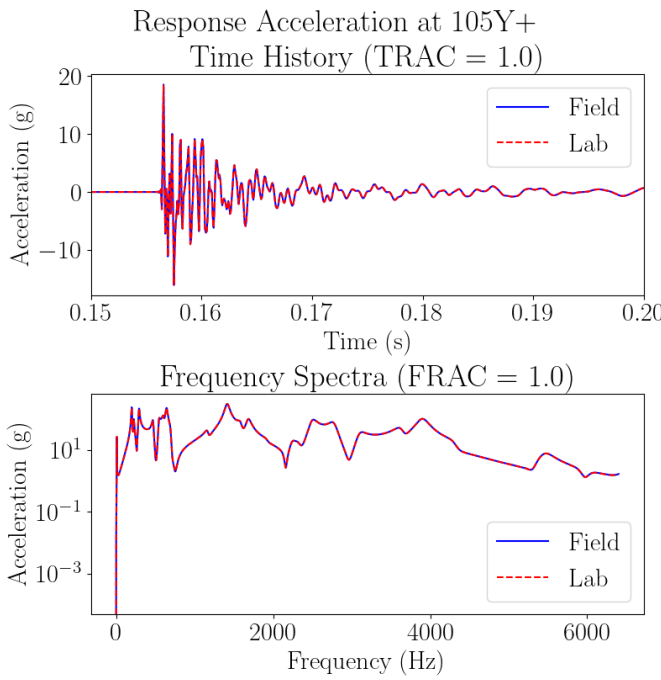


Figure 22: Dual-plate response at 105Y+ compared to reference response.

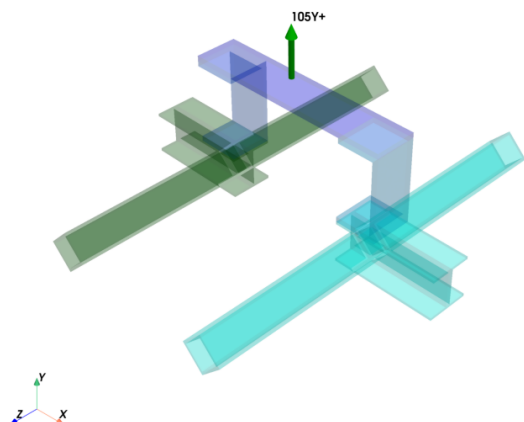
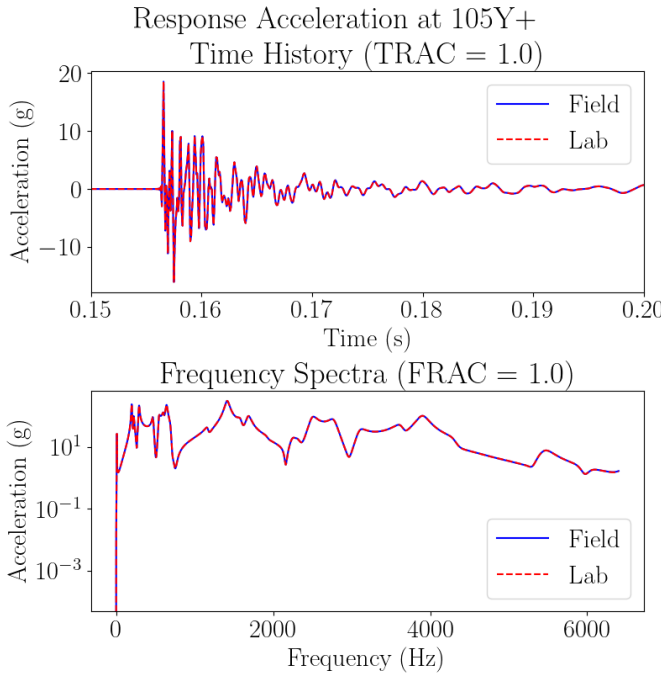


Figure 23: Optimized response at 105Y+ compared to reference response.

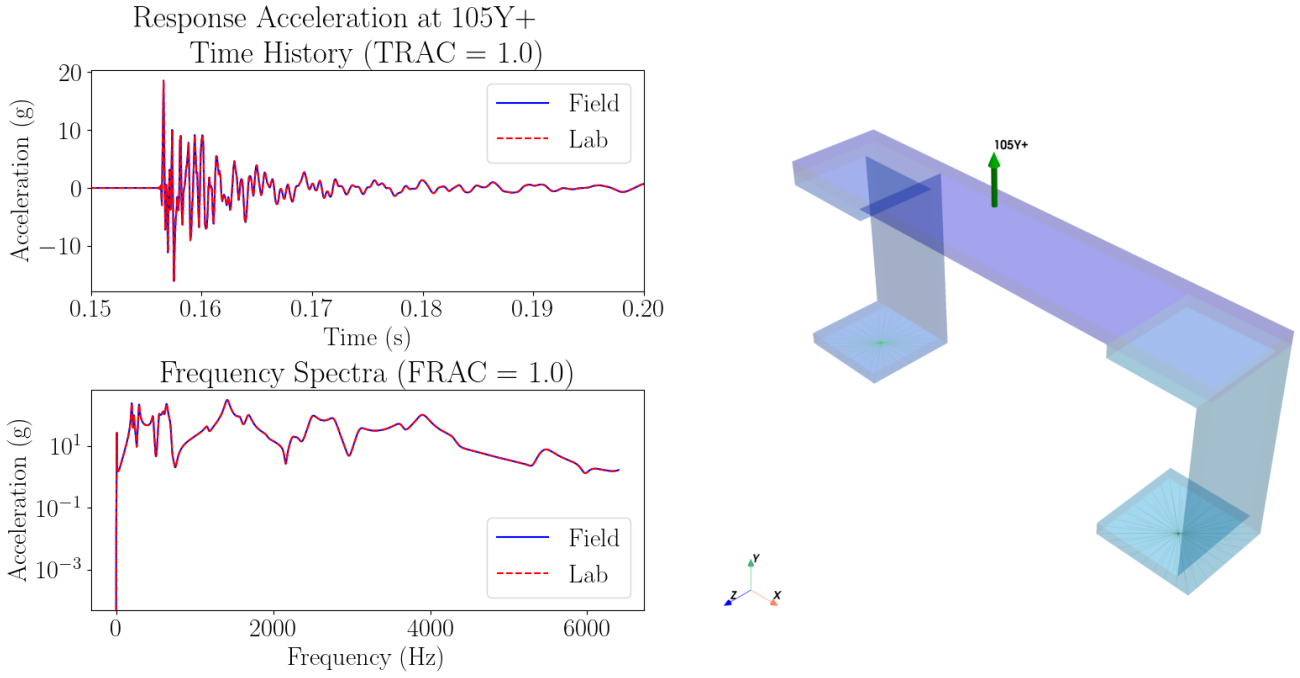


Figure 24: Component response at 105Y+ compared to reference response.

### 5.6 Design Vibration Test Stand

A versatile yet relatively rigid test stand was designed that is capable of holding 12 shakers in appropriate locations for each of the proposed designs. The design of the test stand is shown to demonstrate that a test setups such as the ones proposed in this paper are physically realizable. A more detailed discussion of the design considerations and experimental setup will be discussed in a subsequent paper. A rendering of the test stand is shown in Figure 25 and a zoomed image of the same design in Figure 26.

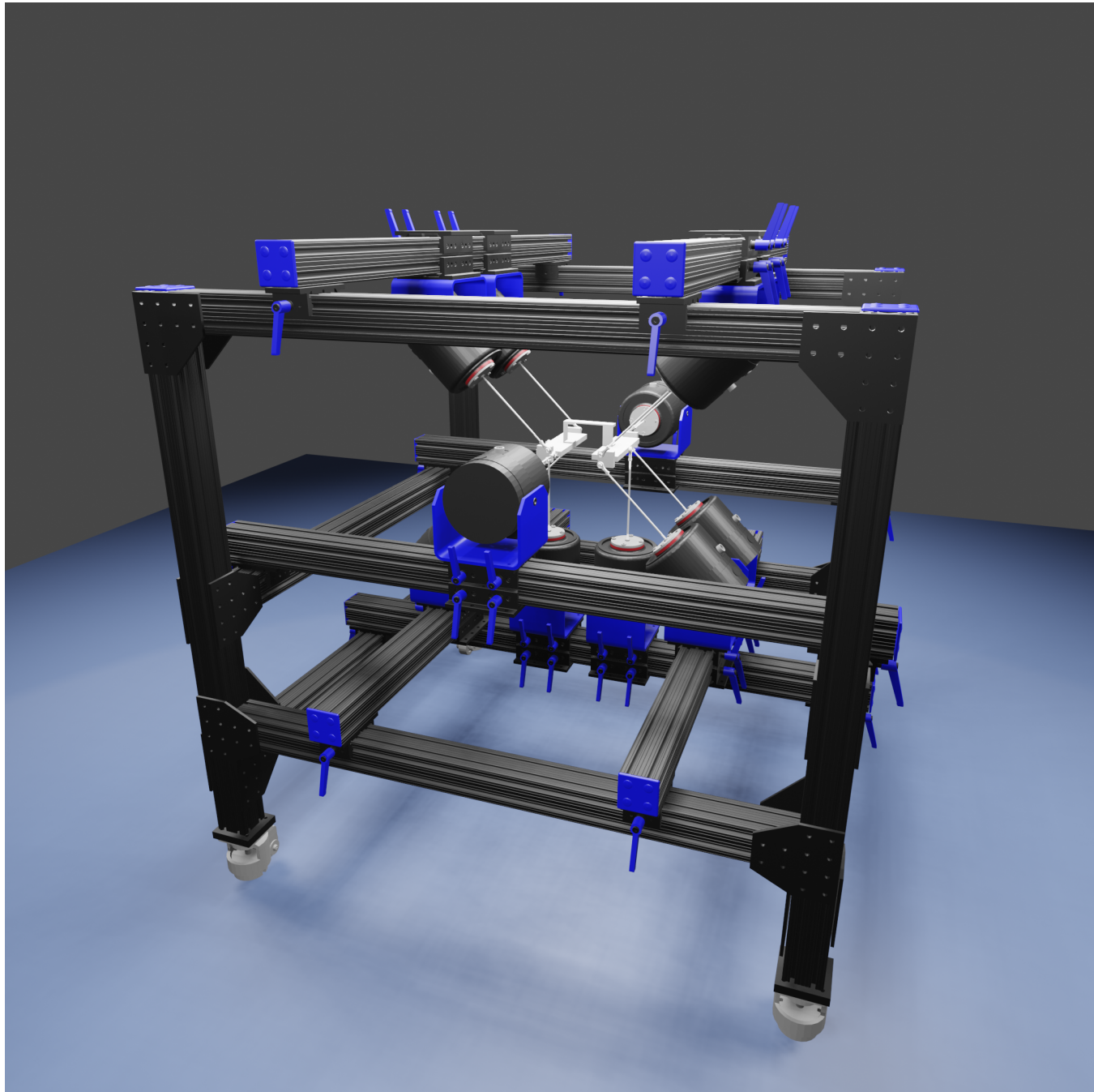


Figure 25: Test setup design for dual-plate fixture design.

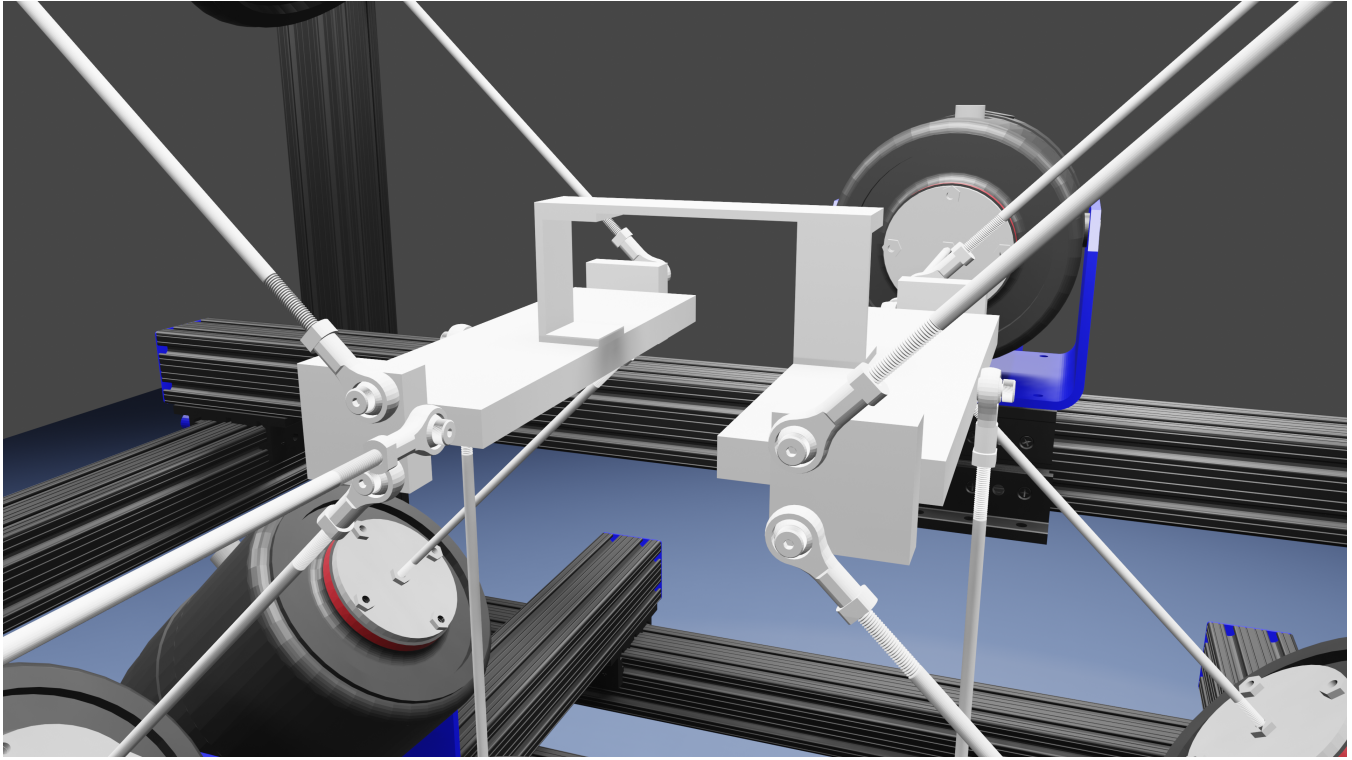


Figure 26: Zoomed view of test setup design for dual-plate fixture design.

## 6 FUTURE WORK

While the methodology demonstrated in this paper addresses some issues with traditional approaches to vibration test design, some areas could use further understanding and development. Specifically there are two aspects to the test setup that were not addressed in this paper.

The first area that was not addressed is optimizing the placement of control accelerometers for the vibration test. In general, the control accelerometers need to be placed such that they are sufficiently conditioned to distinguish the connection forces to the component. Additionally the shakers need to be placed in a manner in which they are sufficiently conditioned to excite all the connection degrees of freedom to the component. In this study, engineering judgement was used to complete both of these tasks, but a quantifiable metric would be preferred in the future.

The second area that was not addressed in this study was the minimization of the rank of the solution utilized. Again engineering judgement was used to produce the assumption that 12 connection degrees of freedom would be sufficient to replicate the component response for a reasonable frequency bandwidth, but there is a possibility that less could be used to achieve a similar result. A singular value decomposition of the connection forces might be able to indicate a reduced rank for the control problem without degrading the results.

## 7 CONCLUSIONS

This paper demonstrates an analytical example of a MIMO vibration test design process with the goal of replicating a structure-born vibration environment of a component in a laboratory setting using different boundary conditions. The methods utilized result in a test design that analytically is capable of replicating the vibration environment because it is designed in a way to ensure that the connection forces acting on the component are replicated thereby compensating for any boundary condition differences between field and laboratory. This paper demonstrates four design concepts in which shaker force magnitudes decrease as the fixture approaches a more optimized solution of being lightweight and stiff in the load path to the component.

## 8 REFERENCES

- [1] David E Soine, Richard J Jones, Julie M Harvie, Troy J Skousen, and Tyler F Schoenherr. “Designing hardware for the boundary condition round robin challenge”. In *Topics in Modal Analysis & Testing, Volume 9*, pages 119–126. Springer, 2019.
- [2] Brandon Zwink. *Dynamic Response Matching from Field to Laboratory Replication Methodology*. PhD thesis, University of Massachusetts Lowell, 2020.
- [3] Jesus M Reyes-Blanco. *Adjustment of input excitation to account for fixture-test article dynamic coupling effects*. PhD thesis, University of Massachusetts Lowell, 2017.
- [4] Philip Matthew Daborn. *Smarter dynamic testing of critical structures*. PhD thesis, University of Bristol, 2014.
- [5] Daniel P Rohe. “Sdynpy: A structural dynamics python library”. In *Proceedings of IMAC 2023*, Austin, TX, February 2023.